Laser-Assisted Room-Temperature Film Growth Using a Constrained Pulsed Nozzle Expansion

Alexander Demchuk, John J. Cahill, and Brent Koplitz*

Department of Chemistry, Tulane University, New Orleans, Louisiana 70118

Received November 9, 1999. Revised Manuscript Received July 18, 2000

Results are presented on a method that uses laser-assisted reactivity in a constrained gas expansion to facilitate film growth. The 193 nm output of an ArF excimer laser is focused through a hole in a substrate into a gas pulse consisting of trimethylamine−alane (TMMA). As shown by mass spectral data, laser irradiation of the TMAA clearly results in significant gas-phase reactivity. While no discernible film growth takes place in the absence of laser radiation, the laser readily brings about film growth on a silicon substrate, even though the substrate is held at room temperature and no laser/substrate interactions occur. Atomic force microscopy is used to investigate the surface morphology present in different regions of the deposited film, and chemical composition in those regions is investigated with Auger electron spectroscopy.

Introduction

High-powered lasers have long held promise as vehicles for influencing the growth of thin films. As ablation sources, excimer lasers in particular have found utility as a means of generating thin films, a good example being the production of superconducting films.[1] In contrast, direct irradiation of a deposition substrate in the presence of a metalorganic precursor(s) can result in the growth of metallic as well as semiconducting thin films.[2−4] In our research group, a longstanding goal has been to use lasers in understandable ways, not only to study laser-assisted chemical reactivity but to correlate this reactivity with thin-film properties. One motivation for the work is to discover routes by which true room-temperature growth conditions can be achieved when metalorganic precursors are used. Here, not only is there a lack of active heating of the growth substrate, but no laser/substrate interactions are introduced either.

Procedurally, we seek to capitalize on advances in pulsed nozzle strategies and pulsed excimer laser technology while keeping laser/substrate interactions to a minimum. In our approach, pulsed nozzles are used as gas sources that feed into a constraining nozzle extender that effectively functions as a transient microreactor. The laser is used to initiate reactivity. Previous work in our laboratory has focused on laser-initiated reactivity in such constrained environments.[5,6] In these experiments, dual pulsed nozzles involving group III and group V metalorganic precursors such as trimethylgallium or triethylgallium and NH_3 were utilized. Photoactivation of both NH_3 and the gallium-containing species was observed. In the current paper, $H_3Al{:}N(CH_3)_3$ (trimethylamine−alane) is employed as a single precursor to explore laser-initiated reactivity with the motivation being to bring about thin-film deposition. Recently, trimethylamine−alane (TMAA) and dimethylethylamine−alane (DMEAA) have been used as Al sources in the chemical vapor deposition (CVD) of high-purity thin films of Al.[7−10] Lewis acid−base adducts such as TMAA are sufficiently volatile at room temperature to produce high deposition rates while decomposing at temperatures as low as 100 °C.[11] Consequently, such precursors have been employed to achieve high-purity Al film growth via pyrolytic CVD or laser CVD through the direct laser irradiation of the substrate.[4,9,12,13] In the present studies, TMAA is cracked in the gas phase by the 193 nm laser output, and films are readily deposited in the absence of any external heating or laser/substrate interactions.

Four features of this work are emphasized at this time. (1) Mass spectral data show that the laser-induced chemistry is "macroscopic" in the sense that a significant portion (∼20−30%) of the parent molecules are being activated. (2) The effects of the laser can be readily monitored with respect to photoactivation as well as subsequent reactivity, i.e., the formation of new com-

(1) Foltyn, S. R.; Meunchhausen, R. E.; Dye, R. C.; Wu, X. D.; Luo, L.; Cooke, D. W.; Taber, R. C. *Appl. Phys. Lett.* **1991**, *59*, 1374.
(2) Baum, T. H.; Larson, C. E.; Jackson, R. L. *Appl. Phys. Lett.* **1989**, *55*, 1264.
(3) Linne, C. J.; Coombe, R. D. *Appl. Phys. Lett.* **1998**, *72*, 88.
(4) Han, J.; Jensen, K. F.; Senzaki, Y.; Gladfelter, W. L. *Appl. Phys. Lett.* **1994**, *64*, 425.
(5) Demchuk, A.; Porter, J.; Beuscher, A.; Dilkey, A.; Koplitz, B. *Chem. Phys. Lett.* **1998**, *283*, 213.
(6) Demchuk, A.; Porter, J.; Koplitz, B. *J. Phys. Chem. A* **1998**, *102*, 8841.
(7) Gross, M. E.; Fleming, C. G.; Cheung, K. P.; Heimbrook, L. A. *J. Appl. Phys*. **1991**, *69*, 2589.
(8) Frigo, D. M.; Van Eijden, G. J. M.; Reuvers, P. J.; Smit, C. J. *Chem. Mater*. **1994**, *6*, 190.
(9) Gladfelter, W. L.; Boyd, D. C.; Jensen, K. F. *Chem. Mater.* **1989**, *1*, 339.
(10) Simmonds, M. G.; Phillips, E. C.; Hwang, J.-W.; Gladfelter, W. L. *Chemtronics* **1991**, *5*, 155.
(11) Gross, M. E.; Harriot, L. R.; Opila, R. L. *J. Appl. Phys*. **1990**, 68, 4820.
(12) Hwang, S.; Byun, D.; Glass, J. A.; Robertson, B.; Spencer, J. T.; Datta, S.; Dowben, P. A. *Mater. Sci. Eng*. **1995**, *B30*, L5.
(13) Glass, J. A.; Hwang, S.; Datta, S.; Robertson, B.; Spencer, J. T. *J. Phys. Chem. Solids*. **1996**, *57*, 563.

10.1021/cm9907209 CCC: $19.00 © 2000 American Chemical Society
Published on Web 09/21/2000

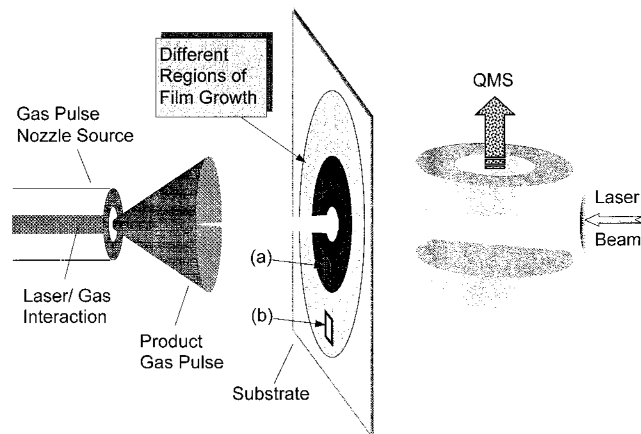

Figure 1. Depiction of experimental apparatus and deposition setup. Labels (a) and (b) identify the regions of growth examined in Figures 4 and 5, respectively.

plexes in the expansion. (3) The deposition of the films can be correlated with laser-induced reactivity within the expansion. (4) The method is general and can be applied to a number of precursor systems including two, three, and four component mixtures.

Experimental Section

A depiction of the experimental apparatus is shown in Figure 1. The system consists of a high vacuum chamber (base pressure $\sim 10^{-7}$ Torr) equipped with a quadrupole mass spectrometer (QMS) and a specialized pulsed nozzle source that has been described elsewhere.[5,6] The TMAA sample (Aldrich; solid powder; vapor pressure of 1.1 Torr at 19 °C) is placed in a small glass vessel wrapped with heating tape and attached to the inlet of the pulsed nozzle system. Introduction of TMAA into the high-vacuum chamber occurs via the nozzle assembly using the vapor pressure of TMAA along with the addition of mild heat ($\sim$30 °C). The result is a pulsed flow of TMAA vapor that is injected into the reaction region of the nozzle assembly. Note that the nozzle itself is kept simply at room temperature. For these experiments, the opening time of the pulsed valve was adjusted to be $\sim$1−2 ms with a repetition rate of 10 Hz.

To initiate chemistry, the 193 nm output from an ArF excimer laser (Lambda Physik Compex 205) is moderately focused with a quartz lens (fl = 250 mm) into the mixing/reaction region of the nozzle through a hole (typically 2−3 mm diameter) in the deposition substrate. As shown in Figure 1, the laser beam and the pulsed expansion are in counterpropagating directions; moreover, the throat of the nozzle expansion region, the hole in the substrate, and the ionization region of the QMS lie on the same axis along which the laser beam travels. A delay generator (Stanford Research Systems) controls the timing between the laser and the pulsed nozzle. Laser beam energies are measured using a Gentec ED-200L joulemeter placed inside the deposition chamber, and these energies varied between 1 and 12 mJ depending on the desired fluence. The delay time between sample injection and laser pulse is typically $\sim$10 ms, and the reaction products formed within the nozzle/reaction zone are mass analyzed with the QMS (Extrel MEXM2000) after passing through the hole in the substrate.

Thin-film deposition experiments were performed under various conditions and laser fluences. The films were deposited on four 1 × 1 cm square silicon substrates mounted on a sheet of copper and centered around a hole drilled in the sheet. The silicon substrates were prepared simply by washing in methanol to remove organic material, so the actual deposition surface was the native oxide layer. The substrates were positioned in the deposition chamber approximately 10 mm from the end of the pulsed nozzle (see Figure 1). This substrate configuration permits the cluster expansion to spray onto the substrates and through the hole so that deposition can occur while data on the laser-induced reactivity can be monitored by the QMS. As shown, the hole also permits passage of the laser beam. Deposition times were typically 2 h with the system running at 10 Hz. The films were then removed from the chamber and transported to separate instruments for analysis.

Atomic force microscopy (AFM) measurements were conducted to examine surface morphology. The samples were imaged with a Nanoscope III atomic force microscope (Digital Instruments) under ambient conditions. All images were taken in contact mode using a 150 × 150 μm scan head and integral silicon nitride tip on a cantilever with a spring constant of 0.12 N/m. The tips have spherical geometry with a radius of approximately 25 nm as determined after deconvolution of the tip size from features of known dimensions on a calibration grid. The samples were also examined for chemical composition. After investigation with AFM, the samples were moved to a VG ESCALab. Subsequent to sputtering with a 7 kV argon ion beam to remove surface contaminants, Auger electron spectroscopy (AES) measurements were made in two different surface regions, so one could compare the incorporation of aluminum, carbon, and oxygen in different regions of the film.

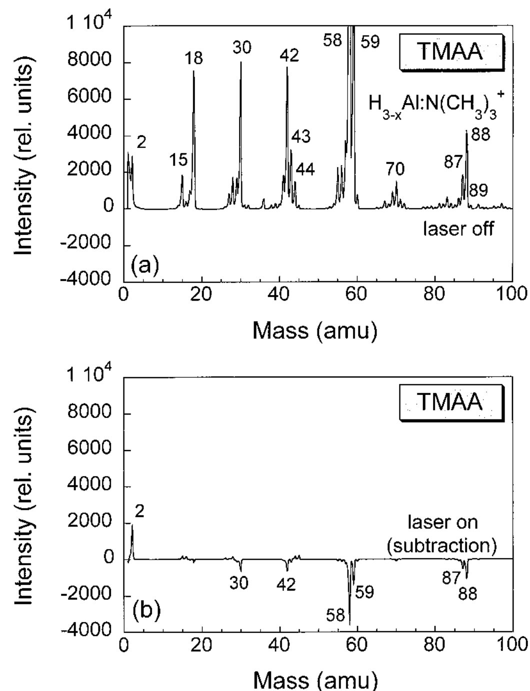

Figure 2. Mass spectra of a TMAA expansion (a) without and (b) with 193 nm laser excitation. In (b), the reported data were obtained after subtraction of the (a) signal that was taken in the absence of laser radiation.

Results and Discussion

The mass spectrum of a TMAA expansion taking place in the absence of laser light is shown in Figure 2a. Ionization is achieved via 70 eV electron impact, and the mass spectrum reveals the presence of a small parent ion feature(s) at masses 87−89 amu with the most intense peak being at mass 88. The dominant daughter ion features at masses 58 and 59 correspond to the trimethylamine portion of TMAA. Mass 30 corresponds to AlH_3^+. In Figures 2b and 3, the effects of laser radiation on the expansion are shown. The spectra are presented in subtraction form; i.e., the signal occurring with no laser radiation present (essentially Figure 2a) is subtracted from the signal generated when the laser beam *does* interact with the expansion. In

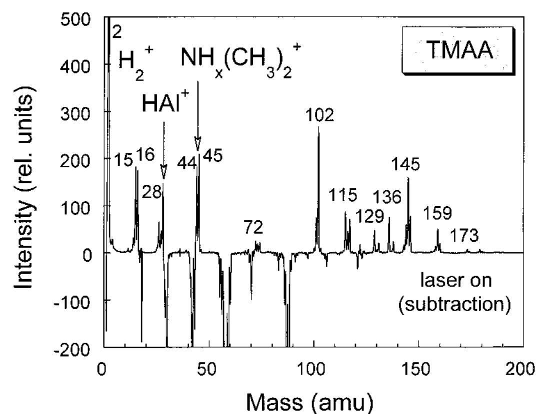

Figure 3. Mass spectra of products formed during TMAA expansion with 193 nm laser excitation. The reported data were obtained after subtraction of the signal that was taken in the absence of laser radiation.

Figure 2b, the presence of major negative peaks clearly indicates that significant numbers of parent molecules are being photolyzed.

The mass spectrum of products formed as a result of laser irradiation is shown in Figure 3. The energy of the laser beam was ~10 mJ at the focusing lens. For lower masses, the presence of a peak at 16 amu suggests that methane is being formed, while a mass of 2 amu indicates that H_2 is also being generated in significant amounts. It is likely that mass 28 is due to AlH^+ occurring either as a parent ion or a daughter fragment, but one cannot rule out the formation of N_2 as a possible source. At the present time, the chemical identities of most of the higher masses are not known. One can speculate that mass 136 is $(AlH)Al_4^+$, but the most prominent peak seen at mass 102 could be represented by $(H_3Al)(H_2Al)_2CH_2^+$ as well as $Al_2O_3^+$ ions. The existence of water as an impurity in the sample handling system is presently still a problem; thus, oxygen as a product must be included as a possibility in any analysis. Such observations have been made previously in analogous systems.[14] Note too that all peaks may also be arising from the fragmentation of higher order species as well as being formed as parent masses. Power dependence studies (not shown) reveal typical saturation behavior[5,6] in the intensities of the higher mass peaks as the photolysis laser energy is increased. One can attribute this behavior to saturation of the TMAA photolysis event within the focal volume.

Upon absorption of a 193 nm (6.4 eV) photon, TMAA has a variety of possible fragmentation pathways available to it. Owing to the very weak Al–N bond in this molecule (estimated to be ~1 eV),[15,16] the logical candidate for the dominant fragmentation event is

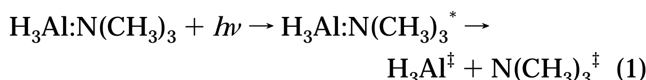

$$H_3Al{:}N(CH_3)_3 + h\nu \rightarrow H_3Al{:}N(CH_3)_3^* \rightarrow H_3Al^{\ddagger} + N(CH_3)_3^{\ddagger} \quad (1)$$

If indeed the initial photochemical step involves this pathway, a dissociating TMAA molecule has ~5.4 eV of energy (plus parent thermal energy) to distribute between its two photofragments. Further fragmentation, collisional reactivity, collisional relaxation, and additional photoreactivity of the fragments are all in competition. One possible outcome in this collisional environment is the reaction of $N(CH_3)_3$ with $H_3Al{:}N(CH_3)_3$ to form $H_3Al{:}(N(CH_3)_3)_2$. Precedence for such a species can be found in the literature.[17–20] Note, however, that tracing these reactive events in such complex systems is difficult. While power and pressure dependence studies as well as wavelength effects can lend insight into the reactive chemistry occurring in these types of systems,[5,6] a detailed photolysis study virtually requires experiments using $D_3Al{:}N(CH_3)_3$ or $H_3Al{:}N(CD_3)_3$. Consequently, our focus in the present work is on determining the viability of achieving macroscopic film growth with the method depicted in Figure 1.

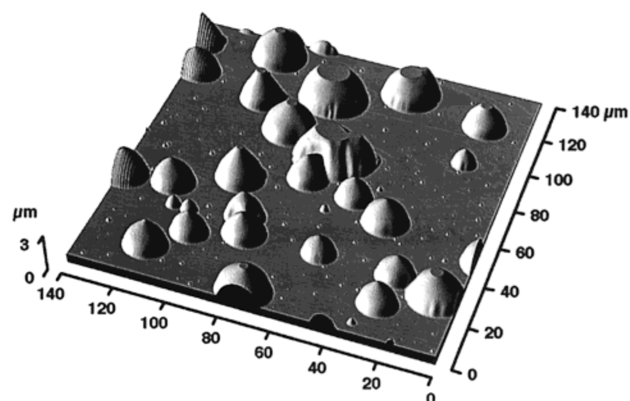

Figure 4. AFM images of the surface morphology of the films deposited with TMAA using 193 nm laser excitation. This region corresponds to the area identified as (b) in Figure 1.

Thin films were grown on silicon substrates over the course of 2 h with the laser operating at 10 Hz and 10 mJ/pulse as measured at the focusing lens. Because of the proximity of the QMS ionizer to the substrate, one can affect the temperature of the deposition substrate itself (up to ~100 °C) simply by operating the ionizer. The films shown in Figures 4 and 5 were taken with the electron impact ionizer off, so the substrate temperature remains at 20 °C. To avoid any unwanted temperature effects, the QMS was only operated prior to deposition and after growth was completed. In the latter case, the substrate was moved from its position close to the QMS while the ionizer was operated.

Note that in the absence of laser radiation, the expanding TMAA molecules produced *no discernible film growth*. In contrast, laser irradiation of the expansion mixture resulted not only in the gas-phase reactivity shown in Figures 2 and 3 but significant film growth was observed on the silicon substrates even when they were kept at 20 °C. Due presumably to the number density gradient present at the gas/substrate interface as one moves further away from the molecular beam axis, the film thickness gradually decreases upon mov-

(14) Simmonds, M. G.; Gladfelter, W. L.; Li, H.; McMurry, P. H. *J. Vac. Sci. Technol. A* **1993**, *11*, 3026.
(15) Elschenbroich, C.; Salzer, A. *Organometallics*; VCH Publisher: New York, 1992.
(16) Thayer, J. S. *Organometallic Chemistry*; VCH Publisher: New York, 1988.
(17) Kodas, T.; Hampden-Smith, M. *The Chemistry of Metal CVD*; VCH Publisher: New York, 1994.
(18) Ruff, J. K.; Hawthorne, M. F. *J. Am. Chem. Soc.* **1960**, *82*, 2141.
(19) Heitsch, C. W. *Nature* **1962**, *195*, 995.
(20) Heitsch, C. W.; Kniseley, R. N. *Spectrochim. Acta* **1963**, *19*, 1385.

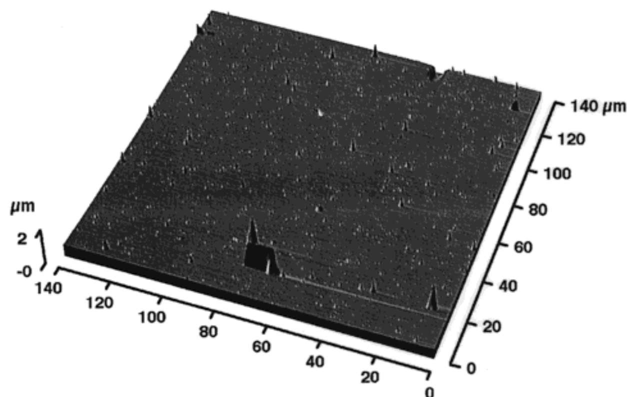

Figure 5. AFM images of the surface morphology of the films deposited with TMAA using 193 nm laser excitation. This region corresponds to the area identified as (a) in Figure 1.

ing away from the molecular beam axis. The actual drop off depends on the laser fluence, precursor backing pressure, and the position of the substrate holder relative to the expansion nozzle. The typical size of the deposited film spot was ~10−15 mm in diameter. As shown in Figure 1, position (a) was ~1 mm from the center hole in the substrate holder, while position (b) was 5 mm away from position (a). The film thickness varies from essentially bare substrate to ~1−2 μm over this region. Consequently, the thin films produced were metallic in appearance but had colored circular deposition bands. In general, increasing the laser fluence produced a thicker film. From a number density perspective, we would expect the deposition rate to decrease if the substrate holder were moved further away from the nozzle. However, we have not yet performed a quantitative investigation in this area.

AFM was used to investigate the surface morphology of the films. Two typical areas showing local and continuous growth are shown in Figures 4 and 5. Their relative positions on the substrate are indicated in Figure 1 by (b) and (a), respectively. The AFM image shown in Figure 4 contains distinct areas of growth with circular rounded shapes that are mostly separated from one another. Note that the flattening observed on some of the dome tops is an upper-limit artifact of the AFM measurement. The small growth regions appear to be sites of nucleation that have not fully coalesced. These symmetric hemispherical shapes appear to grow uniformly until their sizes result in the early merging stages of coalescence. In contrast, as one moves closer to the center of the nozzle expansion stream, growth occurs more quickly most probably due to the increased number density. It is known that the growth of metal film on metal substrates by CVD involves catalytic decomposition of organometallic molecules on the metal surface.[17] In particular, the growth of Al films by CVD using TMAA or DMEAA reveals good selective growth (at low deposition temperatures) on a metal-patterned substrate relative to semiconductor or oxide substrates.[21] This selectivity indicates that the system has a greater propensity for film growth at active Al sites. In our case, whether this propensity arises from simply a greater sticking coefficient or is related to surface mobility with subseqent TMA loss at an active Al-metal

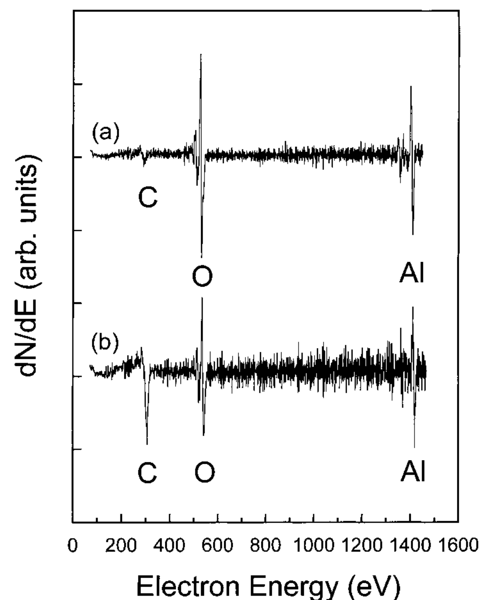

Figure 6. AES spectra for the film deposited in the areas identified as (a) and (b) in Figure 1. After correction for sensitivity factors, the values in (a) are 91, 6, and 3 at. % for Al, O, and C, respectively. In (b), the results are 83, 4, and 13 at. % for Al, O, and C, respectively.

site has not been established. However, it is very likely that the higher number density near the beam axis will lead to continuous growth more quickly; i.e., the entire surface in the region is the more active Al metal.

The results of this faster growth are shown in Figure 5 where one can observe that continuous growth is already taking place. Here, the nucleating islands that marked the earlier stages of growth found in Figure 4 have merged, resulting in a continuous growing layer. When Figures 4 and 5 are examined for roughness, it is necessary to note that the dome-shaped local regions in Figure 4 actually have relatively smooth surfaces. Note also that the flat surface is the substrate. In contrast, the continuous region of Figure 5 does indeed display roughness as evidenced by the many small, pointed formations.

AES was used to study chemical composition in these systems, and the results for the two growth regions are shown in Figure 6. Note that the spectra are presented in derivative mode. Figure 6a shows the continuous film growth area analyzed by AES that is close to the gas expansion axis. After correction for sensitivity factors, the relative abundances are 91, 6, and 3 at. % for Al, O, and C, respectively. In Figure 6b, the local growth area that is ~5 mm further from the nozzle axis was analyzed, and the results are 83, 4, and 13 at. % for Al, O, and C, respectively. One can clearly conclude that the Al/C ratio is higher in the continuous growth region, and we tentatively attribute this increase to different growth conditions in the continuous region. However, the source of the carbon itself must be positively identified before conclusions can be drawn. For example, trace amounts of background pump oil are always present, and the further one goes from the molecular beam axis, the lower the number density of TMAA. Consequently, the relative pump oil contribution will be greater as one goes further from the beam axis. Whether or not it constitutes a significant, measurable source of carbon contamination is not yet clear.

(21) Simmonds, M. G.; Taupin, I.; Gladfelter, W. L. *Chem. Mater.* **1994**, *6*, 935.

While the viability of making films with this method has been demonstrated, the various paths to making good films need to be explored and will be the subject of future investigations. The potentially important parameters to be varied include laser power, laser wavelength, gas pressure, and length of the laser/gas interaction region. Other influences to be examined include substrate rotating and heating as well as annealing of the film after film deposition.

Acknowledgment. We thank Mr. Ivo Doudevski and Professor Dan Schwartz for assistance with the AFM images. Dr. Craig Recatto of Aldrich Co. is acknowledged for help in acquiring the TMAA compound. Financial support from the Department of Energy, the State of Louisiana via the Louisiana Education Quality Support Fund, and the National Science Foundation through Tulane University's Center for Photoinduced Processes is very much appreciated. An equipment donation from AT&T/Lucent is also gratefully noted.

CM9907209